

Cyclohexanone curcumin analogs inhibit the progression of castration-resistant prostate cancer in vitro and in vivo

Sariya Mapoung^{1,2} | Shugo Suzuki³ | Satoshi Fuji³ | Aya Naiki-Ito³ |
Hiroyuki Kato³ | Supachai Yodkeeree^{1,2} | Chitchamai Ovatlarnporn^{4,5} |
Satoru Takahashi³ | Pornngarm Limtrakul (Dejkriengkraikul)^{1,2} 

¹Department of Biochemistry, Faculty of Medicine, Chiang Mai University, Chiang Mai, Thailand

²Center for Research and Development of Natural Products for Health, Chiang Mai University, Chiang Mai, Thailand

³Department of Experimental Pathology and Tumor Biology, Nagoya City University Graduate School of Medical Sciences, Nagoya, Japan

⁴Department of Pharmaceutical Chemistry, Faculty of Pharmaceutical Sciences, Prince of Songkla University, Songkhla, Thailand

⁵Drug Delivery System Excellence Center, Prince of Songkla University, Songkhla, Thailand

Correspondence

Pornngarm Limtrakul (Dejkriengkraikul),
Department of Biochemistry, Faculty of
Medicine, Chiang Mai University, Chiang
Mai, Thailand.

Email: pornngarm.d@cmu.ac.th or pdej@
hotmail.co.th

and

Satoru Takahashi, Department of
Experimental Pathology and Tumor Biology,
Nagoya City University Graduate School of
Medical Sciences, Nagoya, Japan.

Email: sattak@med.nagoya-cu.ac.jp

Funding information

The Association for Promotion of Research
on Risk Assessment, Japan, The Royal
Golden Jubilee Scholarship PhD Program
(RGJ), Thailand (Grant/Award Number:
"PHD/0119/2556"), The National Research
Council of Thailand (NRCT), Thailand
(Grant/Award Number: "2558A10402005"),
The Faculty of Medicine Research Fund,
Chiang Mai University, Thailand (Grant/
Award Number: "113/2559"), The Center
for Research and Development of Natural
Products for Health, Chiang Mai University,
Thailand

Many prostate cancer patients develop resistance to treatment called castration-resistant prostate cancer (CRPC) which is the major cause of recurrence and death. In the present study, four cyclohexanone curcumin analogs were synthesized. Additionally, their anticancer progression activity on CRPC cell lines, PC3 and PLS10 cells, was examined. We first determined their anti-metastasis properties and found that 2,6-bis-(4-hydroxy-3-methoxy-benzylidene)-cyclohexanone (2A) and 2,6-bis-(3,4-dihydroxy-benzylidene)-cyclohexanone (2F) showed higher anti-invasion properties against CRPC cells than curcumin. Analog 2A inhibited both MMP-2 and MMP-9 secretions and activities, whereas analog 2F reduced only MMP activities. These findings suggest that the compounds may inhibit CRPC cell metastasis by decreased extracellular matrix degradation. Analog 2A, the most potent analog, was then subjected to an in vivo study. Similar to curcumin, analog 2A was detectable in the serum of mice at 30 and 60 minutes after i.p. injections. Analog 2A and curcumin (30 mg/kg bodyweight) showed a similar ability to reduce tumor area in lungs of mice that were i.v. injected with PLS10 cells. Additionally, analog 2A showed superior growth inhibitory effect on PLS10 cells than that of curcumin both in vitro and in vivo. The compound inhibited PLS10 cells growth by induction of G1 phase arrest and apoptosis in vitro. Interestingly, analog 2A significantly decreased tumor growth with down-regulation of cell proliferation and angiogenesis in PLS10-bearing mice. Taken together, we could summarize that analog 2A showed promising activities in inhibiting CRPC progression both in vitro and in vivo.

KEYWORDS

anti-cancer, anti-metastasis, curcumin analog, pharmacokinetics, prostate cancer

This is an open access article under the terms of the Creative Commons Attribution-NonCommercial License, which permits use, distribution and reproduction in any medium, provided the original work is properly cited and is not used for commercial purposes.

© 2018 The Authors. *Cancer Science* published by John Wiley & Sons Australia, Ltd on behalf of Japanese Cancer Association.

1 | INTRODUCTION

Prostatectomy and radiation therapy are treatments for low-risk localized prostate cancer. However, treatment of intermediate- and high-risk prostate cancer is supplemented with androgen-deprivation therapy (ADT).¹ A few years after treatment, 40% of patients commonly develop recurrence called castration-resistant prostate cancer (CRPC).¹ In this state, cancer cells are not only resistant to ADT or chemotherapy but are also highly metastatic.² Unfortunately, chemotherapy might not provide survival benefits for CRPC patients and may have an unacceptably high level of toxicity.³ Therefore, finding effective non-toxic compounds that can inhibit cancer metastasis for use in clinical trials to improve survival rates among prostate cancer patients is urgently required.⁴

Curcumin has been used as a food additive and in traditional medicine in many Asian countries. It has a wide range of biological activities, such as anti-inflammatory, anti-oxidative, anti-metastatic, as well as multi-drug resistance reversing properties.⁵⁻⁷ Clinical trials found that curcumin does not display toxicity even at levels of up to 12 g/d.⁸ However, curcumin has not yet been approved as a therapeutic agent because of its limitations, such as poor absorption, limited tissue distribution and rapid metabolism.⁷ Modification of the structure of curcumin is one of the approaches used to improve the bioavailability of curcumin. Mono-carbonyl analogs of curcumin (MAC) in which the β -diketone moiety is replaced by a single carbonyl group have been synthesized and their biological properties and pharmacokinetic profiles studied. Previous studies have reported that *in vitro* stability and *in vivo* pharmacokinetic ability of MAC were higher than those of curcumin.⁹

In the present study, we studied four cyclohexanone curcumin analogs in which the β -diketone moiety was replaced with a cyclohexanone group and the chemical groups on the phenolic ring were modified. We hypothesized that the analogs may provide superior anti-metastatic or anti-cancer growth abilities in androgen-independent human prostate cancer cell lines.

2 | MATERIALS AND METHODS

2.1 | Reagents

Fetal bovine serum and RPMI-1640 were purchased from Gibco BRL Company (Grand Island, NY, USA). Gelatinase A was purchased

from Sigma Chemical Company (St Louis, MO, USA). Modified RIPA lysis buffer, protease inhibitor cocktail and chemiluminescent immunoblotting reagent were obtained from Thermo Fisher Scientific (Rockford, IL, USA).

2.2 | Synthesis of curcumin analogs

Curcumin and four cyclohexanone analogs were prepared as described in our previous study. Briefly after the synthesis reaction, the products were purified by recrystallization in ethanol and characterized by Fourier transform infrared spectroscopy (FTIR) and NMR.¹⁰ Structure of curcumin and the analogs are shown in Figure 1.

2.3 | Cells and cell culture

An androgen-independent human prostate cancer cell line (PC3) was purchased from ATCC. The androgen-independent, androgen receptor-negative rat prostate cancer cell line (PLS10) was established in our laboratory.^{11,12} PC3 and PLS10 cells were cultured in RPMI-1640 with 10% FBS, 5 mmol/L L-glutamine, 50 IU/mL penicillin and 50 mg/mL streptomycin and maintained in a humidified incubator with an atmosphere comprising 95% air and 5% CO₂ at 37°C. When the cells reached 70%-80% confluence, they were harvested and plated either for subsequent passages or for curcumin or its analog treatments.

2.4 | Animals

All animal experiments were carried out under protocols approved by the Institutional Animal Care and Use Committee of Nagoya City University Graduate School of Medical Sciences. Seven-week-old male BALB/c mice and 5-week-old male BALB/c-nu/nu mice were purchased from Charles River Japan Inc. (Atsugi, Japan) and housed in plastic cages with hardwood chip bedding in an air-conditioned room at 23 ± 2°C, and 55 ± 5% humidity with a 12-hour light/dark cycle. An Oriental MF diet (Oriental MF; Oriental Yeast Co., Tokyo, Japan) and distilled water were available *ad libitum*.

2.5 | Cell viability assay

PC3 cells (4.0 × 10³ cells/well) or PLS10 cells (2.0 × 10³ cells/well) were plated in a 96-well plate for 24 hours. After that, various

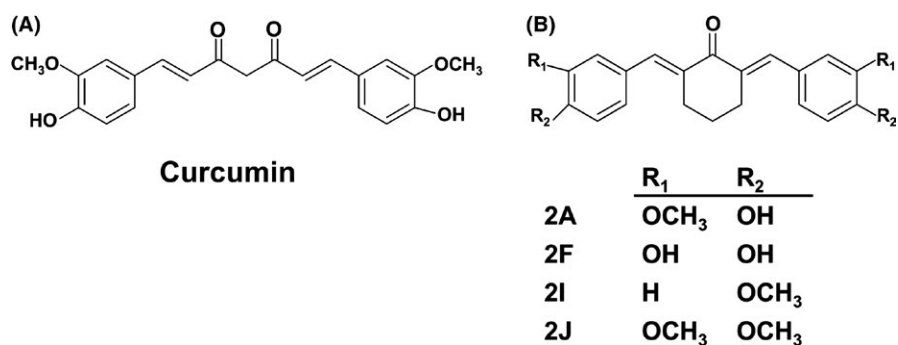


FIGURE 1 Structure of curcumin (A) and its cyclohexanone analogs (B)

concentrations (0–100 $\mu\text{mol/L}$) of curcumin or its analogs were added. The cells were incubated in 5% CO_2 at 37°C for a further 48 hours.

For determination of non-toxic concentration of curcumin or its analogs in FBS-free cultured condition, PC3 (8.0×10^3 cells/well) or PLS10 cells (4.0×10^3 cells/well) were plated and treated with various concentrations (0–10 $\mu\text{mol/L}$) of curcumin or its analogs for 24 hours. Cell viability was determined by MTT colorimetric assay.

2.6 | Cell invasion and migration assays

BD Transwell assay (BD Biosciences, Franklin Lakes, NJ, USA) was used to determine the effects of curcumin or its analogs on PC3 or PLS10 cell invasion and migration. Polyvinylpyrrolidone-free polycarbonate filters (8 $\mu\text{mol/L}$ pore size) were coated with 10 $\mu\text{g/mL}$ fibronectin (migration assay) along with 15 μg matrigel per filter (invasion assay). Fibronectin (10 $\mu\text{g/mL}$) in 0.1% FBS RPMI-1640 or 10% FBS RPMI-1640 was added to the lower chamber as a chemoattractant for PC3 cells or PLS10 cells, respectively. PC3 cells or PLS10 cells (2.0×10^6 cells/well) were plated in the upper chamber with or without curcumin or its analogs at a non-toxic dose (IC_{20}) and incubated for 24 or 48 hours for PC3 cells or PLS10 cells, respectively. Invading or migrating cells were fixed with methanol for 5 minutes and then stained with 0.5% crystal violet in 20% methanol for 30 minutes. Percentages of areas occupied with cells were then determined with IMAGE J 1.410 (National Institute of Mental Health, Bethesda, MD, USA).

2.7 | Gelatin-zymography assay

Matrix metalloproteinase (MMP)-2 and MMP-9 secretions were determined by gelatin-zymography assay. PC3 (5.0×10^6 cells/well) cells were plated into six-well plates and maintained for 24 hours. Cells were then treated with various concentrations of the analogs in FBS-free RPMI-1640 and incubated for 24 hours. Culture supernatant was collected and secretions of MMP-2 and MMP-9 were measured. Briefly, non-heating and non-reducing samples were subjected to SDS-PAGE using a 10% acrylamide gel containing 0.1 mg/mL gelatin. After electrophoresis, gels were washed with 2.5% Triton-X 100 and incubated in activating buffer (50 mmol/L Tris-HCl, 200 mmol/L NaCl, 10 mmol/L CaCl_2 , pH 7.4) for 16 hours.¹³ For MMP-2 and MMP-9 activities, the culture supernatant of FBS-free cultured PC3 cells was subjected to SDS-PAGE as described above. The gel was then cut into slices corresponding to each lane and placed into different tanks containing the analogs dissolved in an activating buffer and incubated for 16 hours. The gels were then stained with 0.1% Coomassie brilliant blue R and destained with 30% methanol and 10% acetic acid. Bands of gelatinolytic activity were analyzed using IMAGE J.

2.8 | In vivo pharmacokinetics

Seven-week-old male BALB/c mice were randomly divided into three groups: control, curcumin- and analog 2A-injection. Mice were i.p. injected with 65% DMSO (control), curcumin or analog

2A (100 mg/kg body weight). Blood samples were collected from each mouse at 0, 30, 60 and 180 minutes after i.p. injection. Concentration of curcumin or analog 2A in serum were determined using HPLC. Briefly, serum (50 μL) was mixed with 1.5 mg/mL trichloroacetic acid in 100 μL acetonitrile and centrifuged at 96.5 g at 4°C for 20 minutes. Supernatant (60 μL) was collected and subjected to HPLC using a reversed phase C18 column (WATERS, Milford, MA, USA). The mobile phase comprised 52% acetonitrile and 48% citric buffer (1% w/v citric acid, pH 3.0) and flow rate was set at 1 mL/min. Detection wavelengths for curcumin and analog 2A were 425 and 340 nm, respectively.^{14,15} Concentration of curcumin or analog 2A in serum was calculated and compared to standard curve (0–3200 ng/mL). Limit of quantification and extraction recovery from plasma of curcumin and analog 2A was 100 ng/mL and 90%, respectively.

2.9 | In vivo anti-metastasis activity

Ten-week-old male BALB/c-nu/nu mice were randomly divided into three groups: control, curcumin (30 mg/kg) and analog 2A (30 mg/kg). Mice in each group received treatment by i.p. injection. Thirty minutes after the treatment, PLS10 cells (1.0×10^6 cells/100 μL) were i.v. injected into the tail vein of each mouse. Body weight of each mouse was measured once a week. Mice were sacrificed at the end of experimental week 2. Organs such as lungs, liver, kidneys and lymph nodes were removed and fixed in 10% buffered formalin. Tissue sections of each organ were stained with H&E. For quantitative analysis of lung metastases, areas of metastasis foci per total area of section were determined under a microscope (BZ-9000; Keyence, Osaka, Japan).

2.10 | In vivo anti-tumor growth activity

We first determined anti-tumor growth activity of analog 2A on PLS10 cells in vitro. PLS10 cells (1.0×10^5 cells/well) were plated into six-well plates overnight. Then, the cells were treated with analog 2A (0–20 $\mu\text{mol/L}$) or curcumin (20 $\mu\text{mol/L}$) for 48 hours. Next, the cell suspension was prepared and stained with propidium iodide (PI) (Guava cell cycle reagent; Guava Technologies, Hayward, CA, USA) or annexin V and 7-AAD (Guava Cell Nexin Reagent; Guava Technologies) according to the manufacturer's protocol. Cell cycle distribution or apoptosis was determined on a Guava PCA Instrument using CytoSoft Software. Cell cycle and apoptosis regulated protein expression were determined by western blot analysis.

In vivo anti-tumor activity of analog 2A compared to curcumin was next examined using 5-week-old male BALB/c-nu/nu mice. Mice were randomly divided into three groups: control, analog 2A, and curcumin. Suspended PLS10 cells ($5 \times 10^5/100 \mu\text{L}$) were s.c. injected into each mouse. After 2 days of injection, mice received vehicle control or 30 mg/kg curcumin or analog 2A by i.p. injection twice a week for 4 weeks. Body weight of each mouse was measured two times per week during the experiment. Tumor volume was measured by

vernier caliper and calculated according to the formula: $0.52 \times (\text{axis } 1 \times \text{axis } 2 \times \text{axis } 3)$. At the end of experimental week 4, mice were sacrificed and primary tumor, lungs, liver, and kidneys were collected and fixed in 10% buffered formalin. Tissue sections of primary tumor and organs were stained with H&E.

2.11 | Western blot analysis

Protein concentration was determined by Bradford method (Thermo Fisher Scientific). For determination of expression levels of protein in lysed cells, the protein was separated by SDS-PAGE using 10% acrylamide gel. Then, the separated proteins were transferred onto nitrocellulose membrane and blocked with 5% (w/v) skim milk in 1× TBS containing 0.3% (v/v) Tween (TBS-T) at room temperature for 1 hour. Membranes were washed twice with TBS-T and incubated with the primary antibody, mouse anti-cyclin D1 (Merck Millipore, Danvers, MA, USA) and rabbit anti-survivin (Cell Signaling Technology, Danvers, MA, USA) at 4°C overnight. After washing five times with TBS-T, membranes were incubated with the HRP-conjugated anti-rabbit or mouse IgG depending on primary antibody (GE Healthcare Bio-sciences, Buckinghamshire, NA, UK) at room temperature for 2 hours and washed with TBS-T five times. Immunoreactive material was then visualized with an enhanced chemiluminescence detection system (GE Healthcare Bio-sciences). To confirm equal protein loading, each membrane was stripped and incubated with mouse anti-β-actin (Sigma-Aldrich).

2.12 | Immunohistochemistry

Paraffin-embedded samples were sectioned and stained with rabbit monoclonal anti-Ki67 (SP6; Acris Antibodies GmbH, Herford, Germany) and rabbit polyclonal anti-CD31 antibodies (Abcam, Cambridge, UK) and sequentially stained with anti-rabbit secondary antibody and avidin-biotin complex. Binding complexes were then visualized with diaminobenzidine. Sections were then counterstained lightly with hematoxylin for microscopic examination. Number of Ki67 staining cells in a minimum of 1000 cells was counted to determine the labeling index. For quantitative analysis of vessel area, CD31-positive areas per total area section were determined under microscopy (BZ-9000).

TABLE 1 Cytotoxicity of curcumin and its cyclohexanone analogs on PC3 cells

Treatment	10% FBS RPMI-1640 ^a		FBS-free RPMI-1640 ^a	
	IC ₂₀ (μmol/L)	IC ₅₀ (μmol/L)	IC ₂₀ (μmol/L)	IC ₅₀ (μmol/L)
Curcumin	16.83 ± 0.76	34.33 ± 4.25	>10.00	>10
2A	4.83 ± 1.04	9.00 ± 0.87***	4.25 ± 0.35	>10
2F	4.33 ± 0.58	6.33 ± 0.76***	3.75 ± 0.35	>10
2I	>100	>100	>10.00	>10
2J	17.00 ± 1.41	>100	1.00 ± 0.00	>10

^aDetermined by MTT assay, the values are presented as mean ± SD of three independent experiments.

****P* < 0.001 vs curcumin.

2.13 | TUNEL assay

Paraffin-embedded samples were sectioned and apoptosis determined in tumor tissue using TUNEL assay (In situ Apoptosis Detection Kit; Takara Bio Inc., Ohtsu, Japan). TUNEL assay was carried out according to the manufacturer's instructions. Number of TUNEL labeled cells in a minimum of 1000 cells was counted to determine the labeling index.

2.14 | Statistical analysis

In the in vitro experiment, experiments were carried out at least in triplicate to confirm reproducibility and presented as mean ± SD. For the in vivo experiment, data are presented as mean ± SEM. Statistical analysis was carried out with Prism version 6.0 software using a *t* test and one-way ANOVA, Dunnett's test or Tukey's multiple comparisons test. Significance was determined at **P* < .05, ***P* < .01 and ****P* < .001.

3 | RESULTS

3.1 | Cytotoxic effects of curcumin and its cyclohexanone analogs on PC3 cells

Results showed that analogs 2A and 2F showed higher toxicity on PC3 than that of curcumin (*P* < 0.001). IC₅₀ of analogs 2A and 2F were 9.00 ± 0.87 and 6.33 ± 0.76 μmol/L, respectively. Meanwhile, analogs 2I and 2J showed no cytotoxicity on PC3 as seen in Table 1. The anti-metastasis effects of curcumin and its analogs should be determined under the FBS-free RPMI-1640 culture condition. Therefore, the cytotoxicity of curcumin and its cyclohexanone analogs in FBS-free RPMI-1640 on PC3 cells was further determined. Results showed that curcumin and its cyclohexanone analogs had varying IC₂₀ and IC₅₀ values, as seen in Table 1. Non-toxic concentration (≥80% cells survival) of curcumin and its analogs [1 μmol/L (2J), 2.5 μmol/L (2F), 5 μmol/L (2A) and 10 μmol/L (curcumin and 2I)] was used to determine their anti-metastasis properties on PC3 cells in all of the following experiments.

3.2 | Effects of curcumin and its analogs on PC3 cells invasion and migration

Results showed that analogs 2F (2.5 μmol/L), 2A (5 μmol/L) and 2I (10 μmol/L) significantly (*P* < .001) decreased PC3 cells invasion by

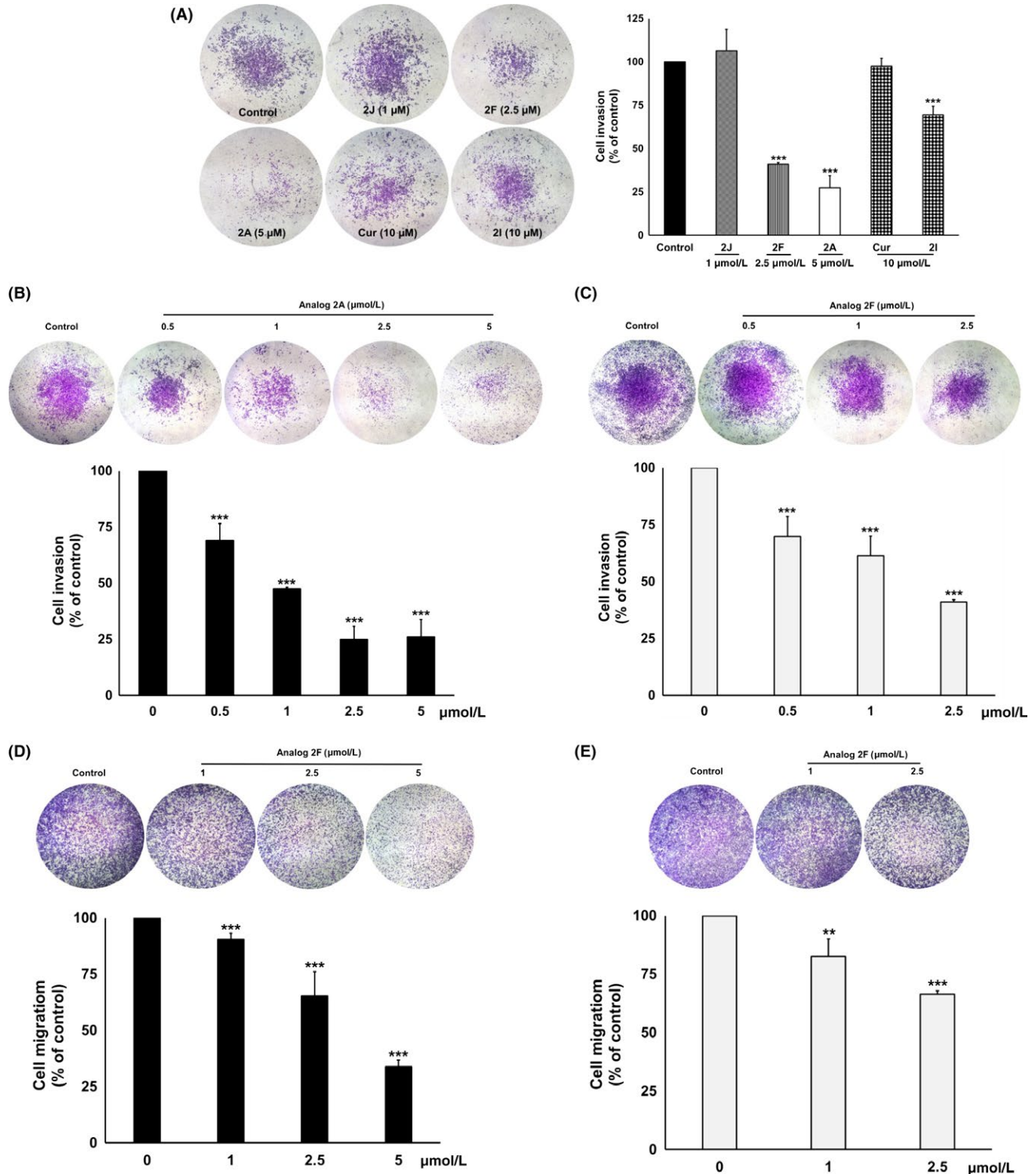


FIGURE 2 Anti-invasion effect of curcumin and its cyclohexanone analogs on PC3 cells. For invasion assay, PC3 cells were treated with a non-toxic concentration of curcumin, or its cyclohexanone analogs (A) or various concentrations of analogs 2A (B) or 2F (C). For migration assay, PC3 cells were treated with analogs 2A (D) and 2F (E). The invading or migrating cells were photographed under phase-contrast microscopy and quantified by IMAGE J software. Data are represented as mean \pm SD of three independent experiments. ** $P < .01$ and *** $P < .001$ vs control

59%, 73% and 30%, respectively, when compared with the vehicle control (Figure 2A). Meanwhile, curcumin (10 $\mu\text{mol/L}$) and analog 2J (1 $\mu\text{mol/L}$) had no effect on PC3 cells invasion. Moreover, analogs 2A and 2F showed a dose-dependent inhibition of PC3 cells

invasion with IC_{50} at $0.93 \pm 0.03 \mu\text{mol/L}$ and $1.70 \pm 0.40 \mu\text{mol/L}$, respectively (Figure 2B,C). Inhibition of PC3 cells migration by analogs 2A and 2F was then determined using transwell migration assay. Results showed that analogs 2A (5 $\mu\text{mol/L}$) and 2F

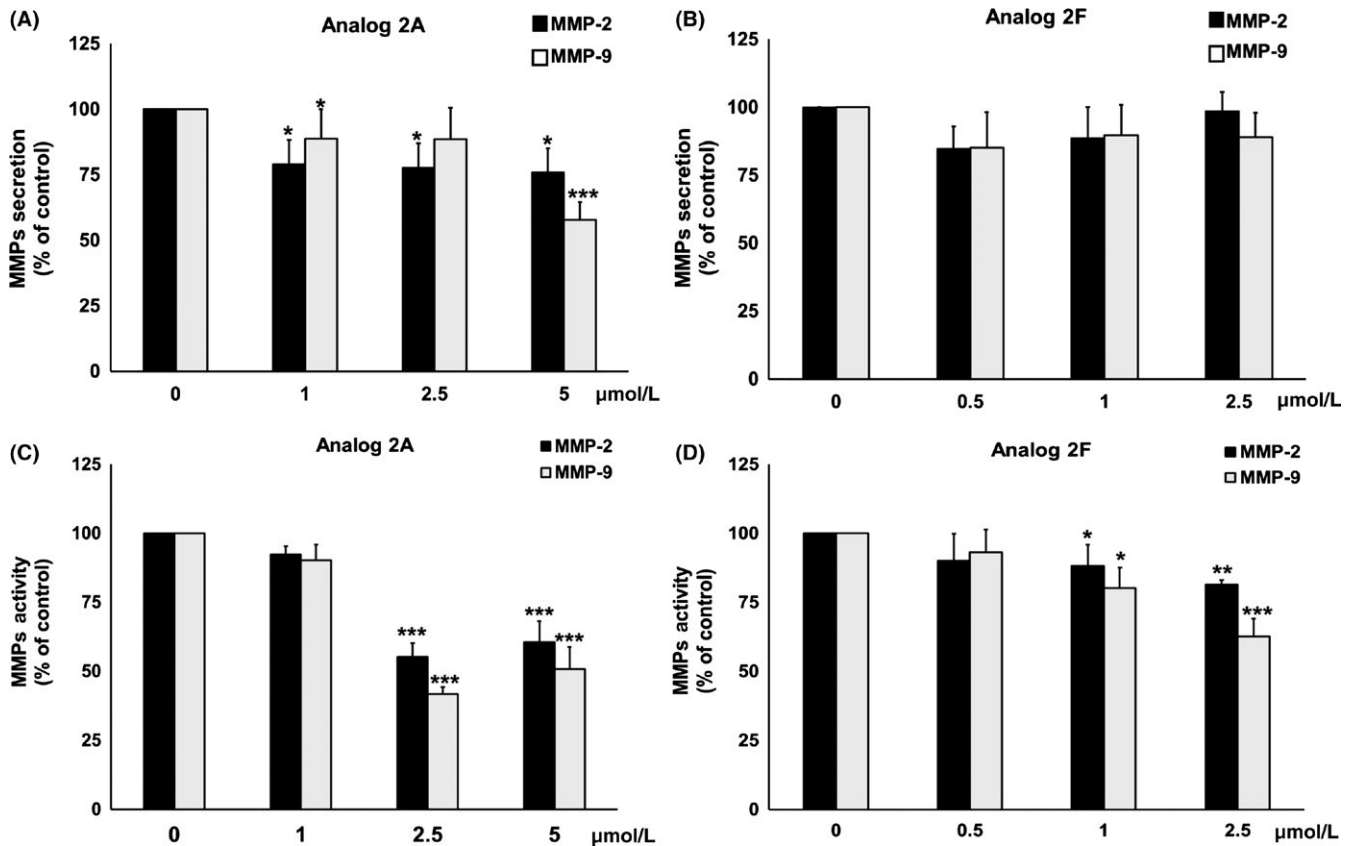


FIGURE 3 Effect of analogs 2A and 2F on secretion (A,B) and activity (C,D) of MMP-2 and MMP-9 in PC3 cells. PC3 cells were incubated with increasing concentrations of analogs 2A (A) or 2F (B) for 24 h. MMP secretion in the culture medium was then determined by gelatin-zymography. For MMP activity, slab gels containing culture medium of PC3 cells were directly incubated with various concentrations of analogs 2A (C) and 2F (B) for 16 h. Level of MMP secretion and activity was quantified by IMAGE J software. Data are represented as mean \pm SD of three independent experiments. * $P < 0.05$, ** $P < 0.01$ and *** $P < .001$ vs control

(2.5 $\mu\text{mol/L}$) significantly inhibited PC3 cells migration by 34% and 66%, respectively, when compared with the vehicle control (Figure 2D,E). These results suggested that the cyclohexanone analogs, 2A and 2F, exerted greater efficacy on the inhibition of PC3 cells metastasis than curcumin.

3.3 | Effects of analogs 2A and 2F on MMP-2 and MMP-9 secretions and activities

We next examined the effects of analogs 2A and 2F on secretions of MMP-2 and MMP-9 which are the major MMP secreted from PC3 cells. It was found that analog 2A significantly decreased MMP-2 (24%) and MMP-9 (42%) secretions from PC3 cells (Figure 3A), whereas MMP-2 and MMP-9 secretions were not significantly decreased by treatment with analog 2F (Figure 3B).

We next determined whether analogs 2A and 2F could reduce the activity of MMP-2 and MMP-9 that is secreted from PC3 cells. It was found that analogs 2A and 2F significantly decreased MMP-2 (39% and 19%, respectively) and MMP-9 (49% and 36%, respectively) activities (Figure 3C,D). According to the results, it could be summarized that analog 2A inhibited both MMP-2 and

MMP-9 secretions and activities, whereas analog 2F inhibited MMP-2 and MMP-9 activities only, leading to a reduction in PC3 cells invasion.

3.4 | Pharmacokinetic results

Analog 2A showed the most potential anti-invasion properties; therefore, it was selected for further in vivo study. In this study, concentrations of curcumin and analog 2A in the serum after i.p. injection were determined. Results showed that the levels of curcumin and analog 2A in the serum were not significantly different. Serum concentration of both compounds appeared mostly at the time interval after 30–60 minutes, and then rapidly declined to normal baseline within 3 hours after the injection, as shown in Figure 4.

3.5 | In vitro anti-metastasis activity of analog 2A in PLS10 cells

Previous results have shown that analog 2A at a low concentration showed strong anti-metastasis potential in vitro and could be found in serum up to 3 hours after i.p. injection. We next

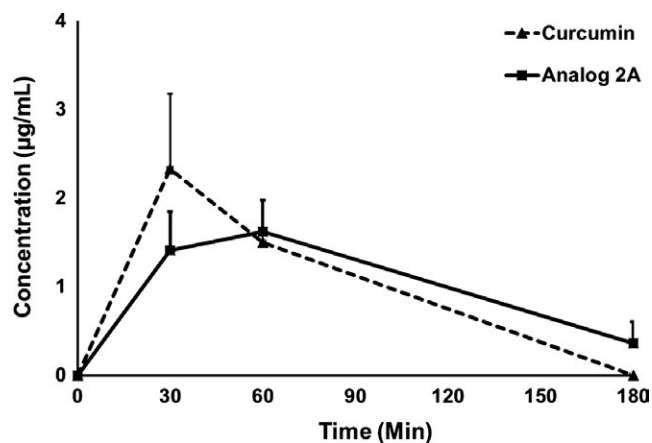


FIGURE 4 Level of serum curcumin and analog 2A in mice after receiving a single dose of curcumin or analog 2A (100 mg/kg) by i.p. injection. The mobile phase comprised 52% acetonitrile and 48% citric buffer. Each point is the mean \pm SE of three or four mice

determined the anti-metastasis effects of this compound in vivo. The PC3 cells xenograft model presented a low incidence of metastasis; therefore, i.v. inoculation of rat-androgen-independent PLS10 cells that exerted a higher incidence of lung metastasis could be used instead.¹⁶

Anti-metastasis properties of analog 2A on PLS10 cells were evaluated in the cell culture model. Results from cytotoxicity testing were similar to those in the PC3 cells. Analog 2A ($IC_{50} = 15.00 \pm 2.83 \mu\text{mol/L}$) showed higher cytotoxicity ($P < .01$) on PLS10 cells than that of curcumin ($IC_{50} = 26.50 \pm 1.80 \mu\text{mol/L}$; data not shown). Non-toxic concentrations of analog 2A (0–2.5 $\mu\text{mol/L}$) or curcumin (2.5 $\mu\text{mol/L}$) were used to determine anti-metastasis influence on PLS10 cells and found that analog 2A significantly inhibited PLS10 cells invasion with IC_{50} at $0.95 \pm 0.07 \mu\text{mol/L}$ ($P < .05$), which is close to the dosage used in the PC3 cells ($IC_{50} = 0.93 \pm 0.03 \mu\text{mol/L}$; $P = .724$; Figure 5A). Additionally, migration was found to have significantly decreased in analog 2A-treated PLS10 cells in a dose-dependent way (Figure 5B). In contrast to PC3 cells, curcumin at 2.5 $\mu\text{mol/L}$ could inhibit both invasion and migration in PLS10 cells. These results confirmed that analog 2A could inhibit the metastasis of both PLS10 cells and PC3 cells.

3.6 | In vivo anti-metastasis activity

In vivo anti-metastasis study found that body and organ (liver and kidneys) weights of curcumin- and analog 2A-treated mice were not significantly different (data not shown). Lung metastasis was 100%, whereas lymph node metastasis was found in only one mouse in the control group (1/7). Lung metastasis area of both curcumin- ($P > .001$) and analog 2A- ($P > .01$) treated mice was significantly decreased when compared to that of the control mice (Figure 5C,D). From the above findings, we can summarize that both curcumin and analog 2A showed similar abilities to inhibit cancer cell metastasis in the animal model.

3.7 | Analog 2A induced cell cycle arrest and apoptosis in PLS10 cells in vitro

In further investigations on the effects of analog 2A and curcumin on tumor growth in the PLS10 xenograft model, we first assessed analog 2A treatment in PLS10 cells on cell cycle progression and apoptosis induction. Analog 2A treatments at 5, 10, 15 and 20 $\mu\text{mol/L}$ resulted in an accumulation of PLS10 cells in G1 phase from 36.13 ± 0.45 in the non-treated control to 37.15 ± 1.20 , 42.93 ± 3.70 , 56.00 ± 4.32 ($P < .001$) and $48.40 \pm 7.89\%$ ($P < .05$), respectively. Curcumin at 20 $\mu\text{mol/L}$ slightly induced G1 arrest in the cells at up to $40.50 \pm 3.05\%$, but not significantly (Figure 6A). We next determined the expression of G1 phase regulatory molecule in PLS10 cells. Analog 2A treatment significantly decreased the expression of cyclin D1 in a dose-dependent way. Meanwhile, curcumin at 20 $\mu\text{mol/L}$ slightly decreased the expression of cyclin D1 in PLS10 cells (Figure 6B).

Furthermore, analog 2A treatment induced PLS10 cell apoptosis in a dose dependent method (Figure 6C). When compared to the control, the apoptotic population increased approximately 1.93- and 3.93- ($P < .001$) fold after treatment with 15 and 20 $\mu\text{mol/L}$ analog 2A, respectively. Meanwhile, 20 $\mu\text{mol/L}$ curcumin did not induce apoptosis because this concentration was lower than that of IC_{50} . Next, the expression of survivin in PLS10 cells after treatment was determined. Analog 2A treatment significantly decreased the expression of survivin in PLS10 cells in a dose-dependent way whereas curcumin did not (Figure 6D). These results indicate that analog 2A inhibited PLS10 growth by induction of cell cycle arrest in G1 phase and apoptosis by downregulation of cyclin D1 and survivin.

3.8 | In vivo inhibition of tumor growth activity

In vivo anti-tumor growth study found that the average size of tumor volume in analog 2A-treated mice was significantly decreased when compared to that of the control mice. Although the tumor volume of curcumin-treated mice was also decreased, it was not significant (Figure 7A). Body and tumor weights of all treated mice were not found to be different when compared to the control group (Table 2). Microscopic observations did not find any lesions in the liver and kidneys among all mice. Immunohistochemistry staining of tumor sections showed that cell proliferation determined by Ki67 labeling index and vessel area determined by CD31 staining were significantly decreased in both the curcumin and analog 2A-treated groups (Figure 7B,C). Meanwhile, apoptosis examined by TUNEL assay tended to be increased in the analog 2A-treated group, but the level was not significant (Figure 7D). The data suggest that curcumin and analog 2A decreased tumor volume by inhibition of cell proliferation and angiogenesis. Additionally, analog 2A could induce apoptosis in the tumor area, which may relate to its superior anti-tumor growth effect when compared to that of curcumin.

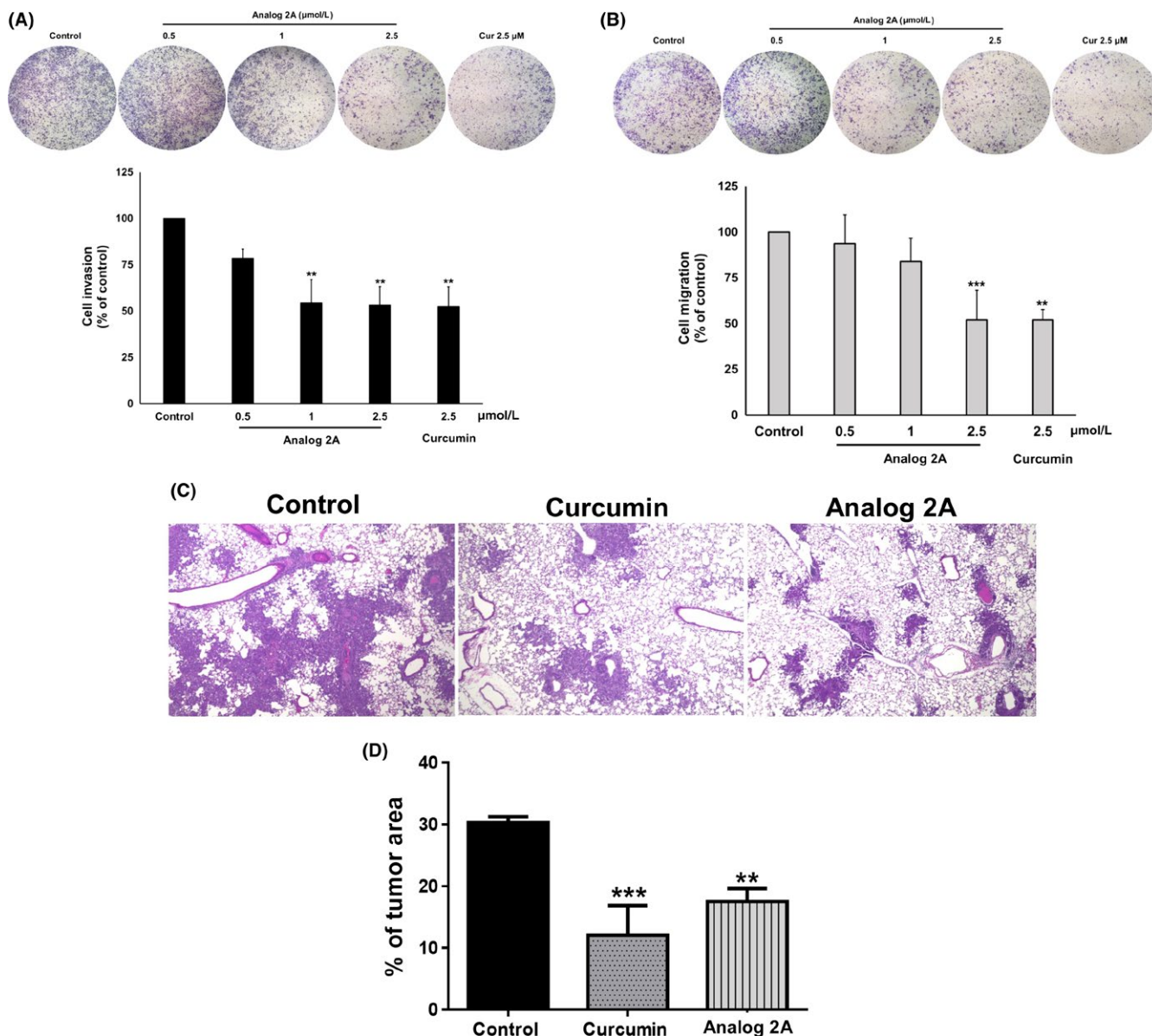


FIGURE 5 Anti-invasion effect of curcumin and analog 2A on PLS10 cells in vitro and in vivo. Invading (A) or migrating (B) ability of PLS10 cells was determined using transwell assay after treatment with curcumin or analog 2A for 48 h. Metastatic cells were photographed under phase-contrast microscopy and quantified by IMAGE J software. Data represent mean \pm SD of three independent experiments. In the in vivo metastasis model, animals were i.p. given 30 mg/kg curcumin or analog 2A. Thirty minutes after treatment, PLS10 cells were injected into the tail vein. Mice were sacrificed at the end of week 2. Representative H&E staining of lung metastases was carried out (C). Lung metastatic foci of each group were determined using a microscope (D). Data are represented as mean \pm SE of each group. ** $P < 0.01$ and *** $P < .001$ vs control

4 | DISCUSSION

Curcumin has been used in clinical trials mainly for cancer but has been hampered by its poor bioavailability.^{7,17} The high reactive potential in pH values above 6.5 and the specific substrate for the reductase of β -diketone moiety resulted in the unstable condition of curcumin both in vitro and in vivo.¹⁸ Replacement of the β -diketone moiety of curcumin with monocarbonyl provides promising pharmacokinetic profiles, improves solubility and stability and enhances selective biological activities.¹⁹ In our previous study, we found that three of the synthetic cyclohexanone curcumin analogs, including analogs 2A, 2F and 2J,

showed higher multidrug resistance-reversal properties than that of curcumin.¹⁰ Another previous study reported that cyclohexanone curcumin analogs exerted a greater level of potency in inducing cell death and inhibiting nuclear factor kappa B (NF- κ B) activity in prostate cancer cells than that of curcumin.²⁰ The cyclohexanone curcumin analogs also showed antioxidant and anti-inflammatory properties both in vitro and in vivo, and there was no acute toxicity after a single oral treatment (2000 mg/kg body weight).²¹

The present study found that analogs 2A and 2F had greater cytotoxicity on PC3 cells than curcumin, whereas analogs 2I and 2J showed no cytotoxicity. The findings suggest that replacement of

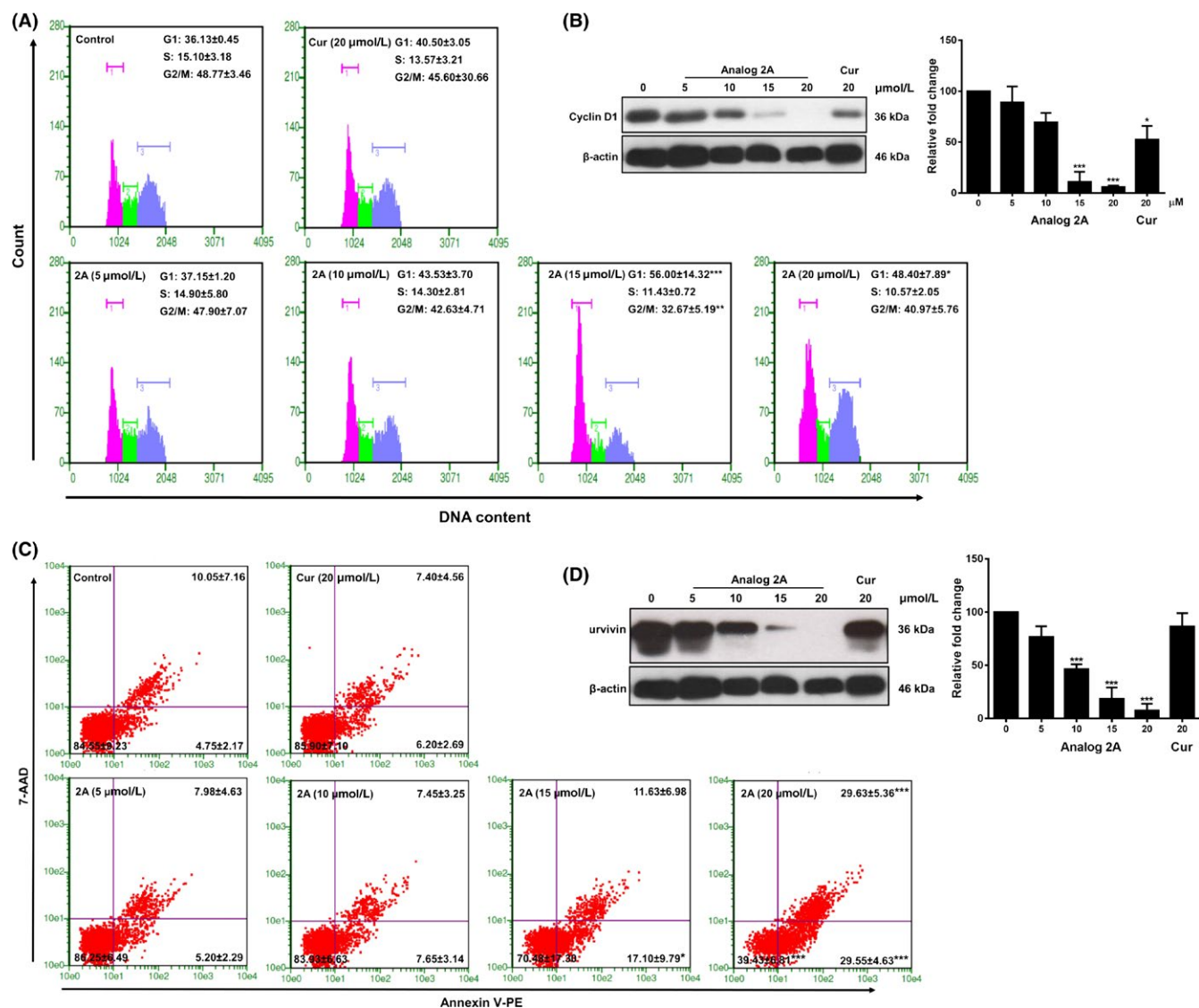


FIGURE 6 Analogue 2A treatment significantly induced G1 phase cell cycle arrest and apoptosis in PLS10 cells. Cells were treated with increasing concentrations of analogue 2A (0–20 μmol/L) and 20 μmol/L curcumin for 48 h. Cells were harvested for analysis of cell cycle distribution (A) and cell cycle regulated protein (B). Apoptotic cells were determined by Guava nexin (C) and protein expression was determined by western blot analysis. Data from a typical experiment are depicted, and similar results were obtained in three independent experiments. Level of protein expression was quantified by IMAGE J software. Data are presented as mean ± SD of three independent experiments. * $P < .05$, ** $P < .01$ and *** $P < .001$ vs control

di-ketone with cyclohexanone, as well as modification of the chemical groups on the phenolic ring, could affect the cytotoxicity of curcumin. The hydroxy group at the R_2 position of each cyclohexanone analog could promote cytotoxicity. Moreover, analogue 2F showed the strongest cytotoxicity effect, which may relate to the hydroxyl group at the R_1 position of this analog.

We found that cyclohexanone curcumin analogs 2A (0.5–5 μmol/L) and 2F (0.5–2.5 μmol/L) showed superior anti-metastatic potency in PC3 cells when compared to that of curcumin (10 μmol/L) and other cyclohexanone analogs. Curcumin and analogue 2A have similar chemical groups on their phenolic rings, but, in analogue 2A, the di-ketone motif of curcumin was replaced with cyclohexanone. These findings suggest that the cyclohexanone group could

promote anti-invasion activity. Additionally, the hydroxyl group at the R_2 position of the phenolic ring may be another factor which promotes anti-invasion activity. Additionally, we found that analogue 2A exerted stronger metastatic inhibition in PC3 cells than that of analogue 2F. The methoxy group at the R_1 position might promote its anti-invasion and anti-migration activities. Although analogue 2J had no effects on the inhibition of cancer cell growth or metastasis, it showed higher multi-drug resistance-reversing properties than those of analogs 2A and 2F.¹⁰ Therefore, differences in the chemical groups on the phenolic ring of curcumin may contribute to certain distinct biological activities.

Previous studies reported that deletion of β -diketone decreased the speed of curcumin metabolism in vivo and that replacement

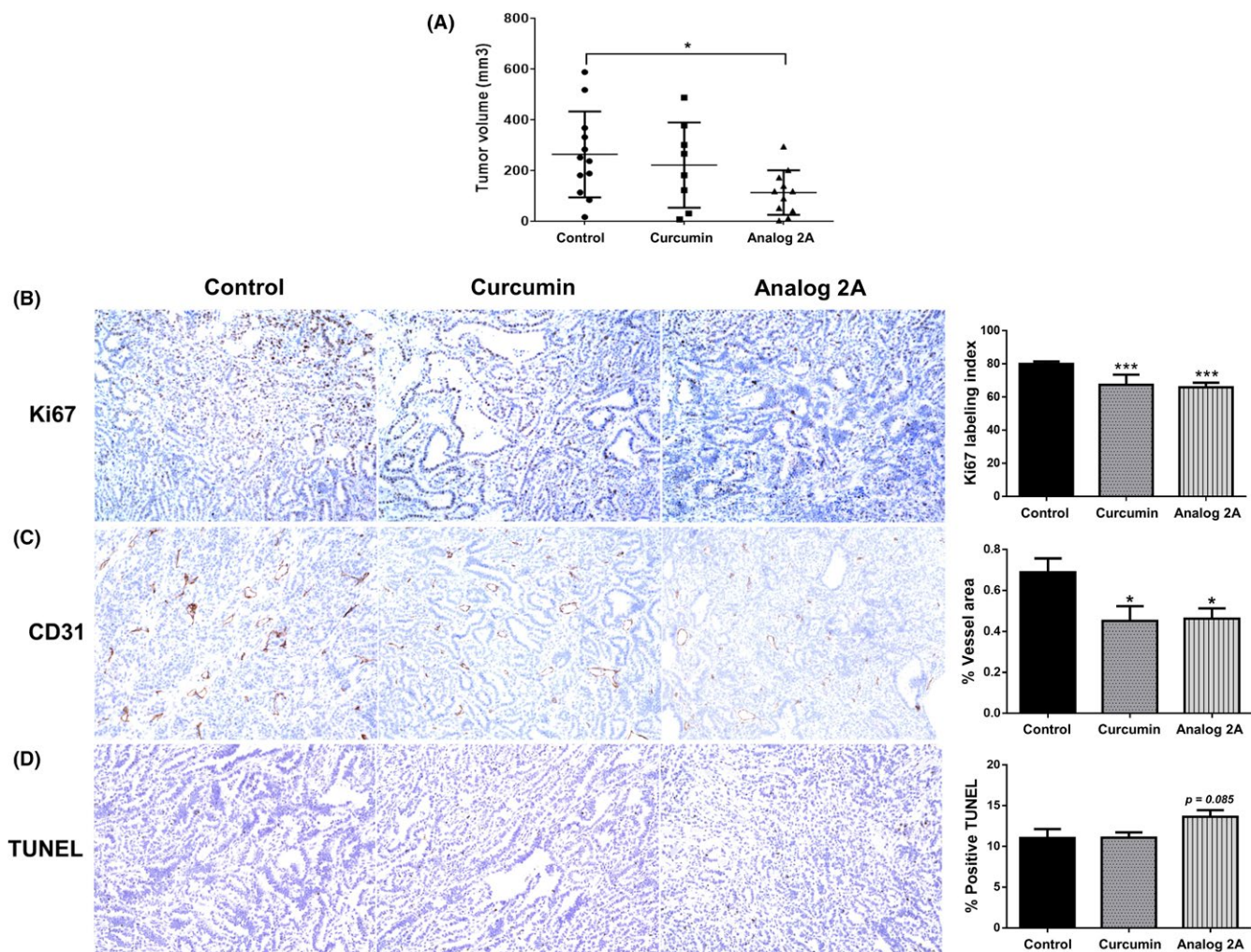


FIGURE 7 Analogue 2A treatment significantly decreased tumor volume. PLS10 cells were s.c. injected into each mouse. The mice then received treatments twice a week for 4 weeks. All mice were then sacrificed, and their tumors were removed and measured for size (A). Tumor section was carried out for immunohistochemistry of Ki67 (B), TUNEL assay (C) and CD31 (D). Data are represented as mean ± SE of each group. **P* < .05 and ****P* < .001 vs control

TABLE 2 Body and organs weights of mice treated long term with curcumin or analogue 2A

Treatment	Body weight (g)		Organs weight (g)		
	Start	End	Liver	L-Kidney	R-Kidney
Control	23.74 ± 0.77	25.23 ± 1.40	1.48 ± 0.14	0.19 ± 0.02	0.20 ± 0.02
Curcumin	23.73 ± 0.75	24.73 ± 2.32	1.45 ± 0.21	0.22 ± 0.07	0.20 ± 0.02
Analogue 2A	23.47 ± 0.72	23.52 ± 2.00	1.37 ± 0.18	0.19 ± 0.01	0.18 ± 0.04

of β-diketone with acetone improved the pharmacokinetic profile of curcumin after oral dosage of 500 mg/kg.¹⁸ The present study found that the pharmacokinetic profile of analogue 2A did not differ from curcumin, suggesting that replacement of β-diketone by the cyclohexanone group might be insufficient to address the pharmacokinetic limitations of curcumin. However, we found that lung metastasis of PLS10 cells was significantly suppressed by both curcumin and analogue 2A treatment by approximately 2.5- and 1.8-fold, respectively. Although the lung metastasis area of the curcumin-treated group was slightly lower than the analogue 2A-treated group,

it was determined to be not significant. Curcumin is rapidly metabolized to dihydrocurcumin and tetrahydrocurcumin, which have anti-metastasis properties.²²⁻²⁴ Metabolism of curcumin might be the one situation that promotes its anti-metastasis activity. Therefore, metabolism of analogue 2A and the biological activities of analogue 2A should be further investigated.

Progression of cancer cells is a complex process, not only in terms of metastasis but also in escaping apoptosis and growth control. We found that analogue 2A exerted a growth-inhibitory effect on PC3 cells (3.8-fold, *P* < .001) and PLS10 cells (1.7- fold, *P* < .01) compared to

curcumin. Previous studies reported that curcumin and its synthetic analogs induced G1 phase arrest in colorectal, colon and prostate cancers²⁵⁻²⁷ and induced G2/M phase arrest in leukemia and cholangiocarcinoma.^{28,29} Therefore, the induction of cell cycle arrest by curcumin and its analogs is specific to each cancer cell type. The present study showed that analog 2A at low dose (15 $\mu\text{mol/L}$) augmented a decrease cyclin D1 expression in PLS10 cells whereas curcumin at high dose (20 $\mu\text{mol/L}$) slightly decreased cyclin D1 expression. The decrease in cyclin D1 level regulated cell cycle arrest in G1 phase.³⁰ Moreover, analog 2A induced apoptosis in PLS10 cells by the decrease in survivin expression in PLS10 cells. Our findings agree with a previous report that demonstrated that cyclohexanone analogs of curcumin had stronger growth inhibitory effect and apoptosis induction in PC3 cells than curcumin, probably by inhibition of NF- κ B transcription activity.²⁰ Taken together, our data suggest that analog 2A inhibited NF- κ B activity which led to growth inhibition and apoptosis stimulation in PLS10 cells.

Furthermore, analog 2A treatments significantly decreased tumor volume when compared to the control group in the PLS10 xenograft model. However, curcumin treatment slightly decreased tumor volume, but not significantly. Immunohistochemistry analyses showed that analog 2A and curcumin treatment decreased cancer cell proliferation and angiogenesis in tumors, although apoptosis induction was slightly increased in the analog 2A-treated group, but not in the curcumin-treated group. Results from in vitro and in vivo studies could be summarized to state that analog 2A may have induced G1 arrest and apoptosis leading to the reduction of tumor volume. Although the pharmacokinetic profile of analog 2A did not differ from curcumin, analog 2A exerted higher anti-tumor growth ability than that of curcumin, particularly on gross examination of tumor volume. Based on the solubility test of curcumin and its analogs, we found that the cyclohexanone analogs showed greater solubility in aqueous solution than did the di-ketone moiety such as curcumin.¹⁰ Therefore, modification of the curcumin structure could assist the limitations of its solubility problem.

In conclusion, our in vitro data showed that the growth inhibitory effects of analog 2A on PC3 and PLS10 cells were more potent than that of curcumin. In the in vivo study, analog 2A showed a significant inhibitory effect on tumor volume whereas curcumin did not. However, for proliferative markers such as Ki67 and in the TUNEL assay, the potency of analog 2A was similar to that of curcumin. For anti-metastasis studies, analog 2A showed similar effects to curcumin in in vivo examination, although analog 2A showed greater anti-invasion effects on PC3 and PLS10 cells in in vitro studies.

ACKNOWLEDGMENTS

This work was supported by Chiang Mai University, Thailand; the National Research Council of Thailand (NRCT) (Grant number 2558A10402005), Thailand; the Faculty of Medicine Research Fund, Chiang Mai University (Grant number 113/2559), Thailand; the Royal Golden Jubilee Scholarship PhD Program (RGJ) (Grant number PHD/0119/2556), Thailand; the Center for Research and

Development of Natural Products for Health, Chiang Mai University, Thailand and the Association for Promotion of Research on Risk Assessment, Japan.

CONFLICTS OF INTEREST

Authors declare no conflicts of interest for this article.

ORCID

Pornngarm Limtrakul (Dejkriengkraikul)  <https://orcid.org/0000-0001-8732-8911>

REFERENCES

1. Fu W, Madan E, Yee M, Zhang H. Progress of molecular targeted therapies for prostate cancers. *Biochem Biophys Acta*. 2012;1825:140-152.
2. Chang YT, Lin TP, Campbell M, et al. REST is a crucial regulator for acquiring EMT-like and stemness phenotypes in hormone-refractory prostate cancer. *Sci Rep*. 2017;7:42795.
3. Chandrasekar T, Yang JC, Gao AC, Evans CP. Mechanisms of resistance in castration-resistant prostate cancer (CRPC). *Transl Androl Urol*. 2015;4:365-380.
4. Lojanapiwat B. Urologic cancer in Thailand. *Jpn J Clin Oncol*. 2015;45:1007-1015.
5. Chearwae W, Anuchapreeda S, Nandigama K, Ambudkar SV, Limtrakul P. Biochemical mechanism of modulation of human P-glycoprotein (ABCB1) by curcumin I, II, and III purified from Turmeric powder. *Biochem Pharmacol*. 2004;68:2043-2052.
6. Cheng TS, Chen WC, Lin YY, et al. Curcumin-targeting pericellular serine protease matriptase role in suppression of prostate cancer cell invasion, tumor growth, and metastasis. *Cancer Prev Res*. 2013;6:495-505.
7. Anand P, Kunnumakkara AB, Newman RA, Aggarwal BB. Bioavailability of curcumin: problems and promises. *Mol Pharm*. 2007;4:807-818.
8. Lao CD, Ruffin MTT, Normolle D, et al. Dose escalation of a curcuminoid formulation. *BMC Complement Altern Med*. 2006;6:10.
9. Shetty D, Kim YJ, Shim H, Snyder JP. Eliminating the heart from the curcumin molecule: monocarbonyl curcumin mimics (MACs). *Molecules*. 2014;20:249-292.
10. Mapoung S, Pitchakarn P, Yodkeeree S, Ovatlarnporn C, Sakorn N, Limtrakul P. Chemosensitizing effects of synthetic curcumin analogs on human multi-drug resistance leukemic cells. *Chem Biol Interact*. 2016;244:140-148.
11. Nakanishi H, Takeuchi S, Kato K, et al. Establishment and characterization of three androgen-independent, metastatic carcinoma cell lines from 3,2'-dimethyl-4-aminobiphenyl-induced prostatic tumors in F344 rats. *Jpn J Cancer Res*. 1996;87:1218-1226.
12. Suzuki S, Naiki-Ito A, Kuno T, et al. Establishment of a syngeneic orthotopic model of prostate cancer in immunocompetent rats. *J Toxicol Pathol*. 2015;28:21-26.
13. Yodkeeree S, Chaiwangyen W, Garbisa S, Limtrakul P. Curcumin, demethoxycurcumin and bisdemethoxycurcumin differentially inhibit cancer cell invasion through the down-regulation of MMPs and uPA. *J Nutr Biochem*. 2009;20:87-95.
14. Punfa W, Suzuki S, Pitchakarn P, et al. Curcumin-loaded PLGA nanoparticles conjugated with anti-P-glycoprotein antibody to overcome multidrug resistance. *Asian Pac J Cancer Prev*. 2014;15:9249-9258.

15. Lee YZ, Ming-Tatt L, Lajis NH, Sulaiman MR, Israf DA, Tham CL. Development and validation of a bioanalytical method for quantification of 2,6-bis-(4-hydroxy-3-methoxybenzylidene)-cyclohexanone (BHMC) in rat plasma. *Molecules*. 2012;17:14555-14564.
16. Pitchakarn P, Suzuki S, Ogawa K, et al. Kuguacin J, a triterpenoid from *Momordica charantia* leaf, modulates the progression of androgen-independent human prostate cancer cell line, PC3. *Food Chem Toxicol*. 2012;50:840-847.
17. Teiten MH, Gaascht F, Eifes S, Dicato M, Diederich M. Chemopreventive potential of curcumin in prostate cancer. *Genes Nutr*. 2010;5:61-74.
18. Liang G, Shao L, Wang Y, et al. Exploration and synthesis of curcumin analogues with improved structural stability both in vitro and in vivo as cytotoxic agents. *Bioorg Med Chem*. 2009;17:2623-2631.
19. Rajamanickam V, Zhu H, Feng C, et al. Novel allylated monocarbonyl analogs of curcumin induce mitotic arrest and apoptosis by reactive oxygen species-mediated endoplasmic reticulum stress and inhibition of STAT3. *Oncotarget*. 2017;8:101112-101129.
20. Wei X, Du ZY, Cui XX, et al. Effects of cyclohexanone analogues of curcumin on growth, apoptosis and NF-kappaB activity in PC-3 human prostate cancer cells. *Oncol Lett*. 2012;4:279-284.
21. Du ZY, Wei X, Huang MT, et al. Anti-proliferative, anti-inflammatory and antioxidant effects of curcumin analogue A(2). *Arch Pharm Res*. 2013;36:1204-1210.
22. Pan MH, Huang TM, Lin JK. Biotransformation of curcumin through reduction and glucuronidation in mice. *Drug Metab Dispos*. 1999;27:486-494.
23. Yodkeeree S, Garbisa S, Limtrakul P. Tetrahydrocurcumin inhibits HT1080 cell migration and invasion via downregulation of MMPs and uPA. *Acta Pharmacol Sin*. 2008;29:853-860.
24. Zhang Y, Liu Y, Zou J, et al. Tetrahydrocurcumin induces mesenchymal-epithelial transition and suppresses angiogenesis by targeting HIF-1alpha and autophagy in human osteosarcoma. *Oncotarget*. 2017;8:91134-91149.
25. Lim TG, Lee SY, Huang Z, et al. Curcumin suppresses proliferation of colon cancer cells by targeting CDK2. *Cancer Prev Res*. 2014;7:466-474.
26. Sha J, Li J, Wang W, et al. Curcumin induces G0/G1 arrest and apoptosis in hormone independent prostate cancer DU-145 cells by down regulating Notch signaling. *Biomed Pharmacother*. 2016;84:177-184.
27. Rajitha B, Belalcazar A, Nagaraju GP, et al. Inhibition of NF-kappaB translocation by curcumin analogs induces G0/G1 arrest and down-regulates thymidylate synthase in colorectal cancer. *Cancer Lett*. 2016;373:227-233.
28. Martinez-Castillo M, Bonilla-Moreno R, Aleman-Lazarini L, et al. A Subpopulation of the K562 Cells Are Killed by Curcumin Treatment after G2/M Arrest and Mitotic Catastrophe. *PLoS ONE*. 2016;11:e0165971.
29. Adams BK, Cai J, Armstrong J, et al. EF24, a novel synthetic curcumin analog, induces apoptosis in cancer cells via a redox-dependent mechanism. *Anticancer Drugs*. 2005;16:263-275.
30. Suzuki S, Pitchakarn P, Sato S, Shirai T, Takahashi S. Apocynin, an NADPH oxidase inhibitor, suppresses progression of prostate cancer via Rac1 dephosphorylation. *Exp Toxicol Pathol*. 2013;65:1035-1041.

How to cite this article: Mapoung S, Suzuki S, Fuji S, et al. Cyclohexanone curcumin analogs inhibit the progression of castration-resistant prostate cancer in vitro and in vivo. *Cancer Sci*. 2019;110:596-607. <https://doi.org/10.1111/cas.13897>